Proceedings 10th NUMGE 2023
10th European Conference on Numerical Methods in Geotechnical Engineering
Zdravkovic L, Kontoe S, Taborda DMG, Tsiampousi A (eds)

https://doi.org/10.53243/NUMGE2023-324

Numerical simulation of soil-structure interaction experiments on shallow founded structures for different mass configurations

M. Koronides[1], S. Kontoe[2,1], L. Zdravković[1], A. Vratsikidis[3], D. Pitilakis[3], A. Anastasiadis[3], D.M. Potts[1]

[1]*Department of* Civil & Environmental Engineering*, Imperial College London, London, UK*
[2]*Department of Civil Engineering, University of Patras, Patra, Greece*
[3]*School of Civil Engineering, Aristotle University of Thessaloniki, Thessaloniki, Greece*

ABSTRACT: Soil-Structure Interaction (SSI) phenomena and foundation rocking can modify the structural response significantly with respect to the response predicted adopting the fixed-base assumption. The importance of SSI and rocking depends, among other factors, on the structural mass and the distribution of static stresses at the soil-foundation interface. Within this context, an experimental campaign was carried out aiming to investigate the SSI effects on the response of a 3m x 3m x 5m steel-framed structure. The prototype structure, called EUROPROTEAS, was founded on a shallow footing at the well-characterised Euroseistest site, while its mass was either 18Mgr or 9Mgr. The present study simulates free vibration experiments, placing particular emphasis on soil nonlinearity and soil-foundation interface. A novel approach to simulate gaps at the soil-foundation interface, foundation rocking and to manipulate interface stresses under static conditions is presented. The three aspects are shown to significantly affect the response, while they are found to be more important for the lighter structure.

Keywords: Soil-structure interaction; Numerical modelling; Interface modelling; Rocking; Interface stresses

1 INTRODUCTION

Soil-Structure Interaction (SSI) phenomena can be associated with the reduction of the fundamental frequency and increase of damping of an SSI system, in relation to an equivalent fixed-base structure. Two of the factors that affect the importance of SSI effects is the soil-to-structure stiffness (σ) and structure-to-soil mass (γ_m) ratios. Analytical and numerical studies (e.g. Veletsos and Nair, 1975; Amorosi *et al.*, 2017) have shown that for seismic problems, a decrease of σ (i.e. a stiffer structure) promotes stronger SSI effects, while the impact of γ_m depends on the value of σ that characterises the SSI system. A system of higher γ_m (i.e. heavier structure) exhibits stronger natural frequency decrease, due to SSI phenomena, than a system of lower γ_m (i.e. lighter structure), provided that the two systems are characterised by the same σ ratio. The heavier SSI system develops higher damping than the lighter one, when the compared systems are characterised by a σ ratio higher than 5. On the contrary, for lower σ ratios, a heavier structure can develop significantly less damping than a lighter one. This behaviour is attributed to the larger inertial forces that are exerted on the heavier structure as well as to its rocking-dominant mode of oscillation, which leads to lower radiation damping.

A clearer relation between structural mass and the importance of SSI effects can be obtained when considering a mechanical load acting on the structure. For this case, a lighter structure is anticipated to exhibit stronger response and potentially stronger foundation rocking. As a result of the increased foundation rocking, the lighter structure is expected to have a more pronounced decrease of the system's fundamental frequency and damping (Koronides et al., 2022a, 2022b).

The present study investigates the dependence of foundation rocking on the structural mass, as well as on the effective normal stress distribution that exists at the soil-foundation interface prior to the excitation. It exploits free and forced vibration strong motion data, collected from real-scale experiments on the frame structure EUROPROTEAS. The structure rests on a surface mat foundation at the Euroseistest site whose geotechnical and geological properties are well-documented by previous studies (e.g. Pitilakis et al., 1999; Pitilakis et al., 2018).

The study presents 3D nonlinear finite element (FE) analyses that simulate free vibration tests on two structural configurations of different mass (9 and 18Mgr). Particular emphasis is placed on modelling the soil-foundation interface. A new hybrid interface model is proposed that extends the model proposed by Koronides et al. (2022a). The model is able to simulate permanent interface gaps, as well as foundation areas that are allowed to detach and re-attach to the soil, as necessary, at various increments of the analyses. A novel approach to manipulate the interface stresses under self-weight conditions is also presented.

2 EXPERIMENTAL CAMPAIGN

2.1 Structure and experimental set-up

The wider experimental programme consisted of free and forced vibration tests on the prototype EUROPROTEAS structure. This frame structure is 5m tall and 3 x 3m in plan, consisting of four steel columns (SHS 150 x 150 x 10mm), steel cross bracing system (L-shape 100 x 100 x 10mm), a mat foundation (9Mgr) and a superstructural mass. Figure 1 depicts the structure's dimensions and the two configurations examined herein. These are fully braced structures with (a) 2 top slabs (FBr_2Ts) and (b) 1 top slab (FBr_1Ts), which have a structural mass of 18Mgr and 9Mgr, respectively.

Both structural configurations were subjected to forced vibration tests, while the FBr_2Ts configuration was also subjected to free vibration tests. During the forced vibration tests, a vibrator was mounted on the top slab and applied unidirectional sinusoidal loads of various magnitudes and frequencies. The free vibration tests comprised a pull-out force that was applied on the top slab at an angle of 9° to the horizontal plane, via a wire rope tensioned by a pulling hoist. The force was measured in-situ by a load cell and when its magnitude reached a desired value, the wire was cut instantaneously, and the structure was free to oscillate until rest. In both types of tests, the excitation force was applied along the NS plane of symmetry, with respect to the coordinate system shown in Figure 1. A comprehensive instrumentation placed on both the structure and the soil surface monitored the response of the SSI system.

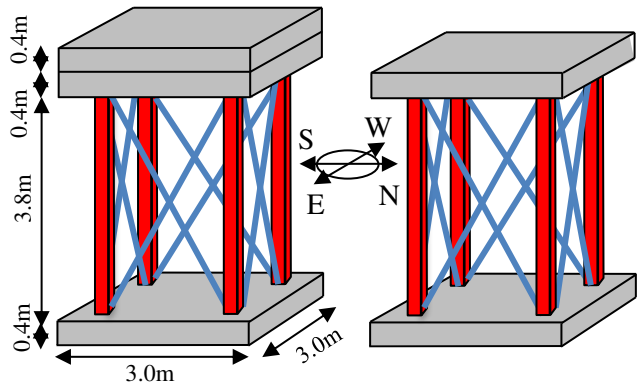

(a) FBr_2Ts (b) FBr_1Ts

Figure 1: EUROPROTEAS' structural configurations: fully braced with (a) 2 top slabs and (b) 1 top slab

2.2 Soil conditions

EUROPROTEAS is located at the TST site, the centre of Euroseistest site, within a valley in Northern Greece, whose geotechnical and geological properties are well documented by previous surveys (e.g. Pitilakis et al., 1999; Pitilakis et al., 2018). Figures 2(a) and (b) present the soil stratigraphy and shear wave velocity profiles, respectively, that resulted from these surveys. The upper soil layers are primarily composed of silty sand and low plasticity clay of very low stiffness, a condition that is expected to accentuate SSI effects.

The geotechnical site characterization involved also soil sampling from different depths below the TST site, some of them are shown in Figure 2(a). Several samples were tested in a resonant column and a cyclic triaxial apparatus to produce stiffness degradation and damping ratio curves (G-γ-D) for the corresponding soil layers.

3 NUMERICAL MODEL

The numerical analyses simulate free vibration tests on both FBr_2Ts and FBr_1Ts structural configurations. The analyses were carried out using the Imperial College Finite Element Program (ICFEP) (Potts and Zdravković, 1999).

3.1 Problem geometry and boundary conditions

Figure 3 presents the 3D mesh, dimensions and some of the boundary conditions for the structural configuration with two top slabs. For the simulation of the one-top slab configuration, an identical mesh was employed without the upper two rows of elements that comprise the 0.4m-thick concrete slab. Exploiting the symmetry of the problem, only half of the domain was modelled.

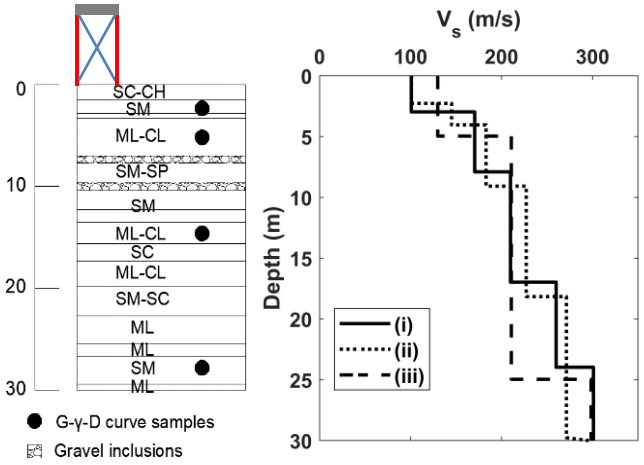

(a) (b)

Figure 2: (a) Soil stratigraphy, (b) shear wave profiles proposed by (i) Pitilakis et al. (1999), (ii) Raptakis et al. (2000) and (iii) Raptakis and Makra (2015)

As per Koronides et al. (2022a, 2022b), the soil domain is modelled with 20-noded brick elements and has dimensions 15 x 7.5 x 6m. The selected model dimensions were found to produce negligible boundary effects on the SSI response, for the examined problem (Koronides, 2023). The 6m deep soil domain is divided into two layers, as illustrated in Figure 3(a). The corner nodes of the bottom boundary of the soil domain are fully fixed, while all nodes at the plane of symmetry (including the soil, base and top slab and braces) are fixed in the out-of plane (y) direction only. Dashpots and springs (Kontoe, 2006) are applied along the normal and

tangential directions on the remaining soil boundary nodes, with the exception of the nodes at the ground surface.

The numerical model explicitly simulates the dimensions of the real structure, as shown in Figure 3(b). The reinforced concrete slabs are modelled with 20-noded brick elements, while the steel columns and braces with 3-noded beam elements. The beam elements of the columns are extended into the brick elements of the slab to achieve moment connection between the columns and slabs. The stiffness of the extended beam elements as well as the damping (ξ) of concrete and steel have been calibrated in Koronides et al. (2022b) and Koronides (2023) against free vibration tests that are not discussed herein. The remaining structural properties are selected according to modern regulations (i.e. British Standards Institution, 2004, 2005). All structural elements are assumed to be linear elastic, while their elastic properties, including Young's modulus (E), Poisson's ratio (ν), density (ρ), cross sectional area (A), moment of inertia (I), torsional constant (J) and target Rayleigh damping (ξ), are shown in Table 1.

The input excitation was applied as a force (F) at a node of top slab that lies in the plane of symmetry, as shown in Figure 3. The simulated experiment applied a force of 15.7kN magnitude, while only half of this value is applied on the numerical model to comply with modelling half of the problem geometry.

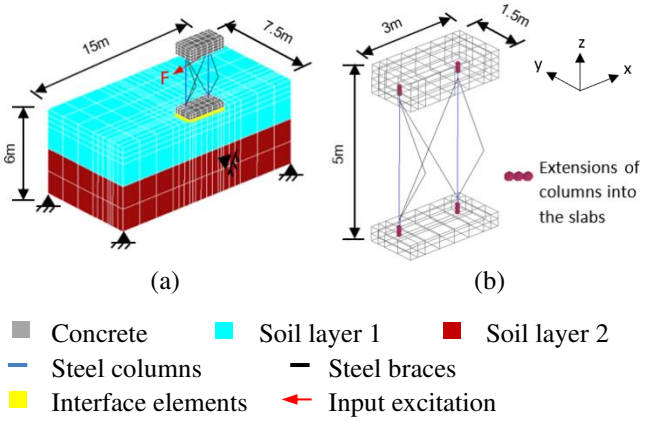

Figure 3: FE mesh, dimensions and the static boundary conditions of the FBr_2Ts configuration: (a) SSI system, (b) Structure

Table 1. Elastic properties of the structural elements

	E (GPa)	ν	ρ (Mgr/m^3)	A (cm^2)	I (cm^4)	J (cm^4)	ξ (%)
Concrete	31	0.2	2.5	-	-	-	1
Braces	200	0.25	7.85	19.2	177	6.97	2
Columns	200	0.25	7.85	54.9	1770	2830	2
Beam elements extended into the foundation	200E4	0.25	0.05	54.9	1770	2830	-
Beam elements extended into the top slab	3	0.25	0.05	54.9	1770	2830	-

3.2 Nonlinear soil model

The first 0.8m of the soil domain is prescribed to behave nonlinearly, while the remaining soil domain is assumed to behave linearly. Koronides (2023) proved that, for this type of problem, the soil nonlinearity, associated with soil hysteresis, is dominated by this superficial layer, in contrast with the remaining layers that mobilised negligible nonlinearity. The small strain stiffness properties, listed in Table 2, were inferred from previous site characterisation studies mentioned earlier (Figure 2(b)).

For the nonlinear soil, the Imperial College Generalised Small Strain Stiffness (IC.G3S) model (Taborda et al., 2016) was used. The calibration of the model's parameters, which determine the G-γ-D curves, is detailed in Koronides (2023). A critical aspect of the calibration process was determining whether to focus on capturing the stiffness or damping curve with greater accuracy. Taborda and Zdravkovic (2012) have shown that if the calibration prioritises the stiffness degradation curve, the soil damping is highly underestimated and highly overestimated at the very low and medium strain range, respectively. As the soil damping is expected to be the dominant factor in the SSI site response, this study prioritises the accurate simulation of damping ratio curves in the small to medium strain range, sacrificing the accurate prediction of stiffness. Figure 4 presents the final calibrated G-γ-D curves input in the analyses, compared with the reference curves. The reference curves were interpreted from the experimental curves, as detailed in Koronides et al. (2022b) and Koronides (2023), where the input parameters of the nonlinear model can be found.

Table 2. Elastic soil properties

	E (Mpa)	ν	ρ (Mgr/m^3)
Layer 1	100	0.25	2.0
Layer 2	186	0.2	2.1

3.3 Types of analyses

Each free vibration simulation consists of three analyses, the Static Self-Weight (StSW), Static Pull-out (StP) and dynamic analyses. The StSW analyses are carried out to create the static conditions of the 'as built' structure, followed by the StP analyses during which the pull-out force was applied statically on the structure in 25 increments. Subsequently, dynamic analyses are undertaken, starting with removing the force in a single increment, followed by the computation of the free oscillation of the SSI system.

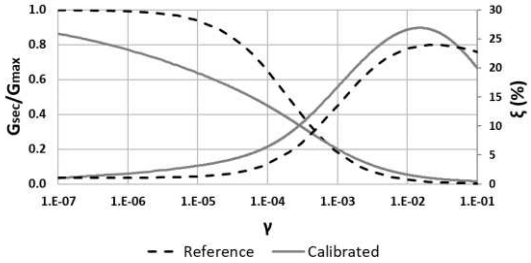

Figure 4: Reference and calibrated stiffness degradation and damping ratio curves

3.4 Soil-foundation interface model

As evidenced from strong motion data and discussed in Koronides (2023), contact imperfections (gaps) between the foundation slab and the soil played a crucial role on the response of the SSI system, as they promoted foundation rocking. Zero thickness interface elements (Day and Potts, 1994) are employed at the soil-foundation interface to allow the simulation of contact imperfections as well as to enable separation between the foundation and the soil beneath. The relative displacement between the soil surface and the foundation base is controlled by the shear (K_s) and normal (K_n) elastic stiffness of the interface elements as well as by their plastic behaviour.

A novel method proposed by Koronides et al. (2022a) adopts the simulation of interface gaps that are able to close and re-open as necessary at subsequent increments of an analysis, as well as the simulation of permanently detached areas. Koronides et al. (2022a, 2022b) have shown that numerical analyses, that model permanently open gaps at interface areas shown in Figure 5, can replicate with sufficient veracity forced and free vibration experiments on the FBr_2Ts structural configuration. The same interface gap configuration is adopted herein. However, the mentioned interface model is not able to allow separation in the interface area that was initially in full contact with the soil. This is addressed by the present study that refines the interface model of the earlier study. A new Hybrid Interface (HYBint), extended from Koronides et al. (2022a), is proposed. The model consists of both elastic and elastoplastic interface elements to effectively model both permanently and temporarily detached foundation areas.

Elastic interface elements of low stiffness (K_s=K_n= 1e2kN/m^3) are employed for the permanently non-contact interface area. For the initial interface contact area, elastoplastic interface elements of high stiffness (K_s=K_n=1e8kN/m^3) are used. For the same area, the interface elements are coupled with an elastoplastic Mohr-Coulomb failure surface which adopts cohesion $c' = 0$ and angle of shearing resistance $\phi' = 30^o$. These interface elements are capable of opening when a mobilized tensile normal stress exceeds the tensile strength set as $c'/\tan\phi'$, which in the current simulations equals zero. While the interface element remains open it has no stiffness and hence no normal or shear stresses are transferred from the foundation to the soil, while any strains occurring are accumulating as normal and shear plastic strains, respectively. The former strains result from differential normal displacements and the latter from differential tangential displacements between the corresponding nodes on the two sides of an interface element, hence having the unit of length.

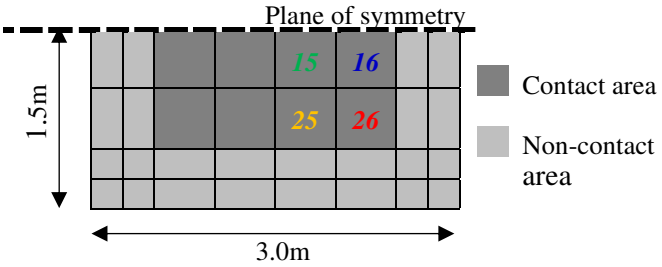

Figure 5: Initial interface contact conditions between the foundation and soil in plan view

The above stiffness values of the interface elements for the contact areas are used in the StP and dynamic analyses. For the static self-weight analyses, the impact of different K_s and K_n values (listed in Table 3) on the response is examined. All analyses adopt K_s=K_n= 1e2kN/m^3 for the non-contact interface areas. The self-weight static analyses, named as StSW8, StSW4 and StSW3, adopt different stiffness values, as shown in Table 3. The interface stiffness, predominantly the normal (K_n) component, affects the normal stresses at the soil-foundation interface, which, as it is subsequently shown, affects the foundation uplift (rocking).

Table 3. Stiffness values, in kN/m^3 units, of interface elements selected for the static self-weight analyses

Analysis name	Contact areas		Non-contact areas	
	K_s	K_n	K_s	K_n
StSW8	1E8	1E8	1E2	1E2
StSW4	1E4	1E4	1E2	1E2
StSW3	1E3	1E3	1E2	1E2

4 RESULTS AND DISCUSSION

Figure 6 presents the contours of effective normal stress (σ'_n) distributions that resulted from the three StSW analyses. As expected, all analyses show almost zero interface σ'_n at the non-contact area. Figure 6(a) presents the stress distribution that resulted from the StSW8 analysis, demonstrating that when a very large stiffness value (i.e. 1e8kN/m^3) is assigned to the contact interface area, the system behaves as a rigid foundation. This is manifested through the large concentration of normal stress around the edges, and especially at the corners, of the foundation contact area. This feature vanishes for smaller interface stiffness values. The StSW4 analysis produced more uniformly distributed σ'_n, with a small stress concentration at the corners (Figure 6(b)). Figure 6(c) shows that the stress concentration disappeared almost completely for the case of the StSW3 analysis.

Figure 7 presents the horizontal response of the top slab in terms of Fourier amplitude spectra, computed by the StSW8, StSW4 and StSW3 analyses, as well as the experimental data, where available. Figure 7(a) shows that the response of the FBr_2Ts structure was marginally affected by the initial distribution of the effective normal stresses at the interface (i.e. under static self-weight). On the contrary, the stress distribution significantly affected the lighter structure (Figure 7(b)), due to higher levels of foundation rocking.

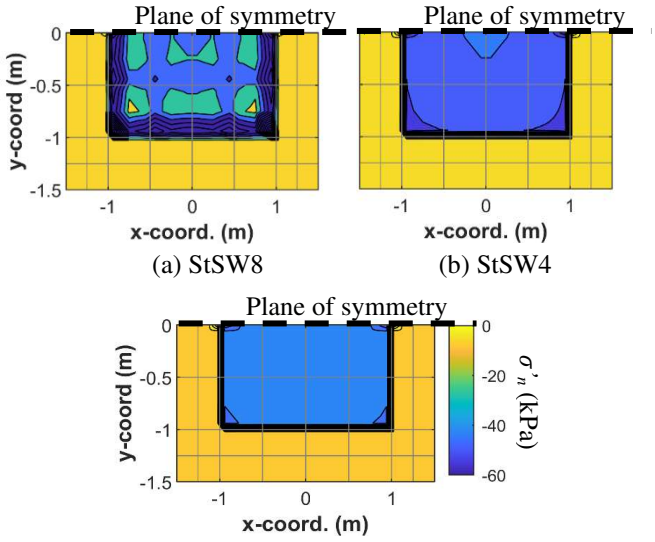

Figure 6: Contours of the effective normal stresses at the soil-foundation interface, under self-weight

Although not shown here, the StSW8 analysed led to zero detachment of the foundation at the initial contact area. Figure 8 presents the normal plastic strains produced by the StSW3 analyses at the integration points of the interface elements numbered in Figure 5. As mentioned earlier, the strains are in units of length and can physically express foundation uplift. Figure 8(a) shows that the foundation of the FBr_2Ts structure detached and re-attached to the soil at limited locations and for a short period of time. The weak opening of the initially closed interface elements implies similar interface contact conditions between the StSW3 and StSW8 analyses, explaining the small difference shown in Figure 7(a). In contrast, the lighter structure exhibited much stronger uplift-attachment alterations at various areas of the interface and for a longer period time. Consequently, for the FBr_1Ts simulations, the choice static stress distribution affects significantly the response of the system, justifying the stronger impact of the static interface stress distribution observed on the lighter structure.

It is concluded that when strong accumulation of stresses exists at the edges of the foundation contact area, these stresses cannot reduce to zero by the structural response, and hence initially closed interface elements are not able to open. On the contrary, when interface normal stresses are well distributed prior to the excitation, the dynamic response of the structure involves more foundation rocking. The stronger foundation rocking that took place during the StSW3 and StSW4 analyses compared to the StSW8 one resulted in smaller contact interface area, making the system more flexible. Also, the decrease of contact area reduces the radiation of waves to the half-space and hence decreases the radiation damping of the SSI system. The above observations justify the smaller fundamental frequency and the stronger response produced by the StSW3 and StSW4 analyses compared to the StSW8 analysis, as indicated by the main peaks in Figure 7b.

The numerical top slab response of the FBr_2Ts structural configuration compares well with the field data (Figure 7(a)). Due to the lack of free vibration experimental data for the FBr_1Ts simulation, Koronides (2023) inferred the fundamental frequency of the system from forced vibration data. This was found to be between 3.25 and 3.5Hz, which is not replicated by the StSW8 and StSW4 analyses that predict a fundamental frequency of 3.92Hz. The StSW3 analysis, though, predicts a frequency (3.52Hz) close to the target one, suggesting that the StSW3 normal stress distribution shown in Figure 6(c) can better represent the distribution that existed prior to the experiments.

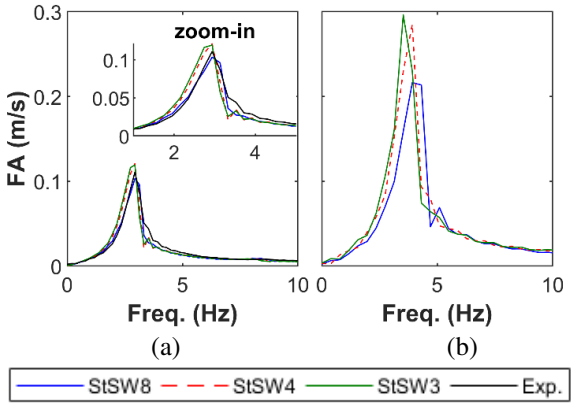

Figure 7: Horizontal top slab response, in terms of Fourier amplitude spectra, computed by (a) FBr_2Ts and (b) FBr_1Ts simulations

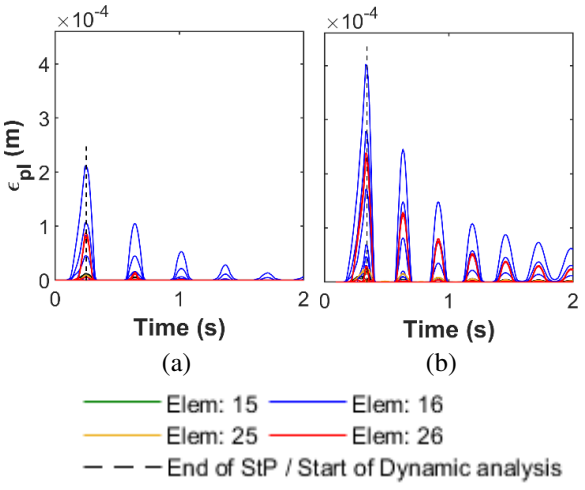

Figure 8: Normal plastic strains computed by StSW3 analyses, that simulate (a) FBr_2Ts and (b) FBr_1Ts free vibration experiments

5 CONCLUSIONS

Three-dimensional SSI numerical analyses, that simulate real-scale experiments of two steel frame structures of different mass, are presented and validated against field data. An interface model (HYBint) that employs both elastic and elastoplastic interface elements, between the shallow foundation and the adjacent soil, was adopted. The elastic elements are used for the simulation of permanently detached interface areas, while the plastic ones for the simulation of initial contact interface areas. In the contact areas, the model allows foundation detachment and re-attachment as necessary during the analysis, simulating rigorously foundation rocking. The present study shows that foundation rocking can be dependent on the distribution of the effective normal stresses (σ'_n) that existed at the soil-foundation interface prior to the application of the excitation load. Foundation rocking can be prohibited by the existence of σ'_n accumulation below the edges of the contact area of the foundation. This σ'_n distribution is normally predicted by FE models below rigid foundations. In this context, a method to alter the distribution is presented herein. It is shown that when normal stresses are more uniformly distributed at the soil-foundation interface, foundation rocking is accentuated. The impact of the σ'_n distribution on the dynamic response is shown to be more pronounced on lighter structures, which are more prone to rotation when the excitation is applied on the structure.

As per Koronides et al. (2022b), the present study demonstrates that foundation rocking can decrease the natural frequencies and radiation damping of SSI systems, under certain circumstances. Finally, results of analyses, that initiate with a different distribution of static σ'_n at the soil-foundation interface, are compared. The analysis that uses the StSW3 stress distribution predicts a system's natural frequency closest to the target one. Thus, for the studied experiments, it is decided that the StSW3 stress distribution can better represent the in-situ conditions.

6 ACKNOWLEDGEMENTS

The experiments were funded by SERA (Seismology and Earthquake Engineering Research Infrastructure Alliance for Europe). The first author wishes to thank Skempton Scholarship, A.G. Leventis Foundation and Cyprus State Scholarship Foundation for their support.

7 REFERENCES

Amorosi, A., Boldini, D. and di Lernia, A. (2017) 'Dynamic soil-structure interaction: A three-dimensional numerical approach and its application to the Lotung case study', *Computers and Geotechnics*, 90, 34–54.

British Standards Institution (2004) *BS EN 1992-1-1:2004. Eurocode 2. Design of concrete structures. General rules and rules for buildings*.

British Standards Institution (2005) *BS EN 1993-1-1:2005, Eurocode 3. Design of steel structures. General rules and rules for buildings*.

Day, R.A. and Potts, D.M. (1994) 'Zero thickness interface elements—numerical stability and application', *International Journal for Numerical and Analytical Methods in Geomechanics*, 18(10), 689–708.

Kontoe, S. (2006) *Developement of time integration schemes and advanced boundary conditions for dynamic geotechnical analysis*. Imperial College London.

Koronides, M. (2023) *Numerical and field investigation of dynamic soil structure interaction at full-scale*. Imperial College London.

Koronides, M., Kontoe, S., Zdravković, L., Vratsikidis, A., Pitilakis, D., Anastasiadis, A. and Potts, D.M. (2022a) 'Numerical simulation of real-scale vibration experiments of a steel frame structure on a shallow foundation', *Proceedings to the 4th iInternational Conference on Performance-based Design in Earthquake Engineering,* (Eds: Wang, L., Zhang, J., Wang, R.)*,* 1119-1127. Cham: Springer International Publishing.

Koronides, M., Kontoe, S., Zdravković, L., Vratsikidis, A., Pitilakis, D., Anastasiadis, A. and Potts, D.M. (2022b) 'Numerical simulations of field soil-structure interaction experiments on a shallow founded steel frame structure', *Proceedings to the 3rd International Conference on Natural Hazards & Infrastructure*.

Pitilakis, D., Rovithis, E., Anastasiadis, A., Vratsikidis, A. and Manakou, M. (2018) 'Field evidence of SSI from full-scale structure testing', *Soil Dynamics and Earthquake Engineering*, 112(March), 89–106.

Pitilakis, K., Raptakis, D., Lontzetidis, K., Tika-Vassilikou, T. and Jongmans, D. (1999) 'Geotechnical and geophysical description of euro-seistest, using field, laboratory tests and moderate strong motion recordings', *Journal of Earthquake Engineering*, 3(3), 381–409.

Potts, D.M. and Zdravković, L. (1999) *Finite element analysis in geotechnical engineering: theory*. Thomas Telford, London.

Raptakis, D., Chávez-García, F.J., Makra, K. and Pitilakis, K. (2000) 'Site effects at Euroseistest-I. Determination of the valley structure and confrontation of observations with 1D analysis', *Soil Dynamics and Earthquake Engineering*, 19(1), 1–22.

Raptakis, D. and Makra, K. (2015) 'Multiple estimates of soil structure at a vertical strong motion array: Understanding uncertainties from different shear wave velocity profiles', *Engineering Geology*, 192, 1–18.

Taborda, D.M.G., Potts, D.M. and Zdravković, L. (2016) 'On the assessment of energy dissipated through hysteresis in finite element analysis', *Computers and Geotechnics*, 71, 180–194.

Taborda, D.M.G. and Zdravkovic, L. (2012) 'Application of a Hill-Climbing technique to the formulation of a new cyclic nonlinear elastic constitutive model', *Computers and Geotechnics*, 43, 80–91.

Veletsos, A.S. and Nair, V.V.D. (1975) 'Seismic interaction of structures on hysteretic foundations', *Journal of the structural division*.